RSC Advances




ROYAL SOCIETY OF CHEMISTRY

www.rsc.org/advances

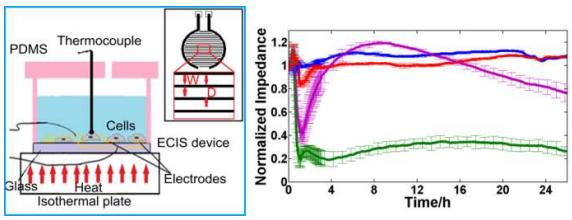


A platform based on ECIS technique was constructed for analyzing heat-cell interactions and further *in-vitro* hyperthermia studies.

# *In-vitro* Hyperthermia Studied in a Continuous Manner Using Electric Impedance Sensing

Xinwu Xie[1,3,4], Ran Liu†[1], Youchun Xu[1,3], Lei Wang[3], Ziyang Lan[1], Weixing Chen[1], Haoran Liu[1], Ying Lu[1,3] and Jing Cheng*[1,2,3,5]

[1] Department of Biomedical Engineering, School of Medicine, Tsinghua University, Beijing 100084, China

[2] Collaborative Innovation Center for Diagnosis and Treatment of Infectious Diseases, The First Affiliated Hospital, College of Medicine, Zhejiang University, Hangzhou 310003, China

[3] National Engineering Research Center for Beijing Biochip Technology, 18 Life Science Parkway, Beijing 102206, China

[4] Institute of Medical Equipment, Academy of Military Medical Science, Tianjin 300161, China

[5] The State Key Laboratory of Biomembrane and Membrane Biotechnology, Tsinghua University, Beijing 100084, China

† This author contributed equally to the first author.

* Correspondence should be addressed to J.C.(jcheng@tsinghua.edu.cn).

Tel: (86)-10-62772239. Fax: (86)-10-80726898.

# Abstract

In this study, a new platform based on electric cell-substrate impedance sensing (ECIS) was constructed for the dynamic monitoring of changes in cells during and after hyperthermia treatments. ECIS profiling was compared with traditional methods for monitoring status of A549 cells under three typical treatment conditions, *i.e.*, 30 min of hyperthermia at 41, 43, and 45 ℃. The impedance value rapidly changed, and severe morphological changes were observed during and after the hyperthermia. The impedance curves revealed that different hyperthermia conditions differentially affected the cells: the 41 ℃ treatment caused a minor decrease in impedance that almost completely recovered in 1-2 h; the 43 ℃ treatment led to a greater decrease in impedance, which also recovered over several hours before slowly decreasing again, possibly indicating apoptosis; the 45 ℃ treatment resulted in the greatest decrease in impedance, which never recovered, possibly indicating rapid necrosis. Further, these three hyperthermia treatment regimens were applied to four additional cell lines. By comparing the impedance curves of different cell lines, we found that cancer cells (HepG2) may be more sensitive to hyperthermia than normal cells (LO2). Moreover, different cancer cell lines (HeLa, MCF-7, A549, and HepG2) exhibited different thermal sensitivities. These results fit previous theories on hyperthermia, demonstrating that the platform established in this study is a useful analytical tool for the in vitro research of thermal therapy, and the dynamic data generated will enable us to examine phenomena and theories.

# Introduction

Recently, several trials have demonstrated that hyperthermia treatment is a useful adjunct to radiotherapy or chemotherapy during the treatment of numerous types of cancers, such as superficial cutaneous tumors, recurrent breast cancer, liver cancer, lung cancer, and cervical carcinoma[1, 2]. To study hyperthermia, most research is conducted *in vitro* to enable accurate application and control of heat to specific cell lines. Previous *in vitro* studies demonstrated that the rate of cell death caused by exposure to heat is exponential and depends on the temperature and exposure time[3]. Typical survival curves plotted by cell viability data usually display a shoulder, which is indicative of a threshold for thermal damage to the cells[4-6]. Generally, hyperthermia with mid-range dose/time combinations induces apoptosis, whereas an excessive dose of heat induces necrosis. However, the mechanism of how hyperthermia affects the cells is not yet fully understood, and the effective thermal dose (the amount of heat required) and the correlated temperature or exposure time for different kinds of cancer still need to be investigated[7]. Previous studies reveal that the cell apoptosis temperature threshold is 43 ℃ for many cell lines, such as HeLa cells[7, 8]. But Lim *et al.*[9] and Shellman *et al.*[10] demonstrate that different temperature thresholds exist for different cell lines. Thus further research on mechanisms is needed to fully utilize and optimize hyperthermia treatments on a particular cancer[11-13].

Various methods have previously been used to perform *in vitro* studies of hyperthermia-induced apoptosis/necrosis at the cellular and molecular levels, including cell viability tests[14], apoptosis staining [15] with a subsequent absorbance detection[16], and caspase assays[10, 17]. Compared to these methods, electrical cell-substrate impedance sensing (ECIS) is

a label-free and non-invasive technique for continuous monitoring of a variety of cell biological processes[18], such as changes in cell spreading and adhesion[19], proliferation[20], migration[21], and apoptosis[22]. With the aid of an automatic sensing system, detection and analyses could be automatic. These merits of ECIS helped us to establish an on-line monitoring system for a non-invasive, dynamic study[23-25]. Further, the high speed sensing system allows us to shorten the detection duration, which makes it possible to detect rapid changes in cellular impedance, for example, the rapid $Ca^{2+}$ concentration changes during hyperthermia can affect impedance [18, 26, 27]. The plotted dynamic curves can provide useful information for choosing the appropriate time point for performing a specific, invasive test, reducing the consumption of time and reagents during pilot experiments. Recently, the ECIS technique was used to measure toxicity of nanoparticles[28, 29], and research stem cell differentiation[30]; the electric impedance sensing chips coupled with hydrogel[31] or microfluidic channels[32] were used for automatic drug diffusion and cytotoxicity research; even an electric impedance sensing chip was fabricated with arrays capturing single cells for single cancer cell migration analysis[21]. Compared to the researches exploring chemical or biological stress on cells, physical stresses on cells studied by ECIS were much less published. Recently an ECIS system was used to investigate the light induced stress changes and the antagonist drugs on retinal cells[22]. Although having been used to study drug-cell[32], compound-cell[19], electric pulses-cell[33, 34], or light-cell[22] interactions, the ECIS technique has never been published to research heat-cell interactions or hyperthermia.

Therefore, impedance profiling could help us to investigate the entire process of a cell's stress reaction, self-repair, and apoptosis or necrosis, which will lead to a deeper

understanding of heat-cell interactions and hyperthermia. In this study, an ECIS system was integrated with a heating and temperature-controlling system aimed at continuously and quantitatively assessing hyperthermia-induced cell apoptosis/necrosis under typical thermal therapy conditions. Cellular status was being monitored by the ECIS system during the entire experiment, especially the commonly used hyperthermia temperatures of 41 ℃, 43 ℃, and 45 ℃. Then, the dynamic impedance curves were verified by means of apoptosis staining, cell viability tests and dynamic live cell morphological observation for a deeper understanding of the process at cellular level. Subsequently, impedance curves of a normal cell line and a cancer cell line derived from a human liver were compared under typical hyperthermia conditions. Finally, the thermal sensitivity of different cancer cell lines, including HeLa, MCF-7, HepG2 and A549 cells, were evaluated with our experimental platform. The impedance curves of these cell lines demonstrated that different cell lines display differences in thermal sensitivity, which will be helpful for mechanistic research and can be applied in clinical hyperthermia treatments in the future.

# Experimental

## 2.1 Materials and reagents

Polydimethylsiloxane (PDMS, Sylgard 184) was supplied by Dow Corning, Inc. (Midland, MI). Fetal bovine serum (FBS) was purchased from PAA Laboratories (Cölbe, Germany). Dulbecco's Modified Eagle's Medium (DMEM) medium, trypsin/EDTA solution, penicillin, and streptomycin were purchased from HyClone Laboratories, Inc. (South Logan, Utah). Propidium iodide was purchased from Invitrogen (Carlsbad, CA). All other reagents were supplied by Sigma-Aldrich (St. Louis, MO).

## 2.2 Cell culture

Five different cell lines (HeLa, MCF-7, A549, HepG2 and LO2) were obtained from the American Type Culture Collection (ATCC, Manassas, VA). The cells were cultured in DMEM supplemented with 10% FBS, 100 U/ml penicillin, and 0.1mg/ml streptomycin and incubated at 37 ℃ in a humidified incubator containing a 5% $CO_2$ atmosphere. Cells for seeding were prepared as a monodisperse cell suspension using standard tissue culture techniques with 0.25% trypsin containing 0.53 mM EDTA.

## 2.3 Experiment platform for in vitro hyperthermia and ECIS measurement

The platform (see Fig. 1) was comprised of three isothermal plates (800 W, POLISH P-20, Jinglianghe Technology Co., Ltd, Shenzhen, China), a self-developed ECIS system, 32 thermocouples (K type, OMEGA Engineering, Inc. Stamford, CT), a data acquisition system (34970A, Agilent Technologies, Santa Clara, CA), and a $CO_2$ incubator (SANYO Electric Biomedical Co., Ltd, Osaka, Japan). The isothermal platform's temperature was controlled by a Proportion Integration Differentiation (PID) controller, which accurately maintained the temperature (with an accuracy of 0.5 ℃) at a set value. Cells seeded on the ECIS devices were independently heated by the isothermal plates. The ECIS system included a NI DAQ card (PCI-6110, National Instruments Corp., Austin, TX), a self-developed amplifying circuit, a PC with data processing software developed by LabVIEW (National Instruments Corp.), and four self-developed ECIS devices with temperature sensing function. The impedance measurement was performed using the amplifying circuit cooperating with the PCI-6110 card, which could provide AC probe signals and acquire the responding voltage signals for 32 sensing channels simultaneously. The self-developed software was employed to control the

measurements, process the data, and display the impedance values. Other than our previous published system[23], the ECIS signal acquiring and processing procedure was optimized to detect and process all 32 channels' impedance in a minimum time frame of 16 s. This allows us to monitor cells' rapid change processes such as heat-induced cell stress reaction. The ECIS device was composed of four elements: a printed circuit board (PCB), a glass chip, a PDMS cell culture cavity, and a pair of thermocouple in the PDMS cover. This eight-channel device had two independent glass chips, each with four cavities formed by PDMS. There were gold interdigital electrodes on the glass chip, which had been fabricated according to microelectronic processing methods. The parameters' optimization of these electrodes (width = 20 μm, distance = 100 μm) and details of the fabrication of this device are published in our previous studies[35-37]. The thermocouples were fixed by the cover and their sensitive probes were immerged into the culture medium, on the same layer of the adherent cells (see Fig.1c) so that the temperatures detected and controlled were the real-time value that cells experienced.

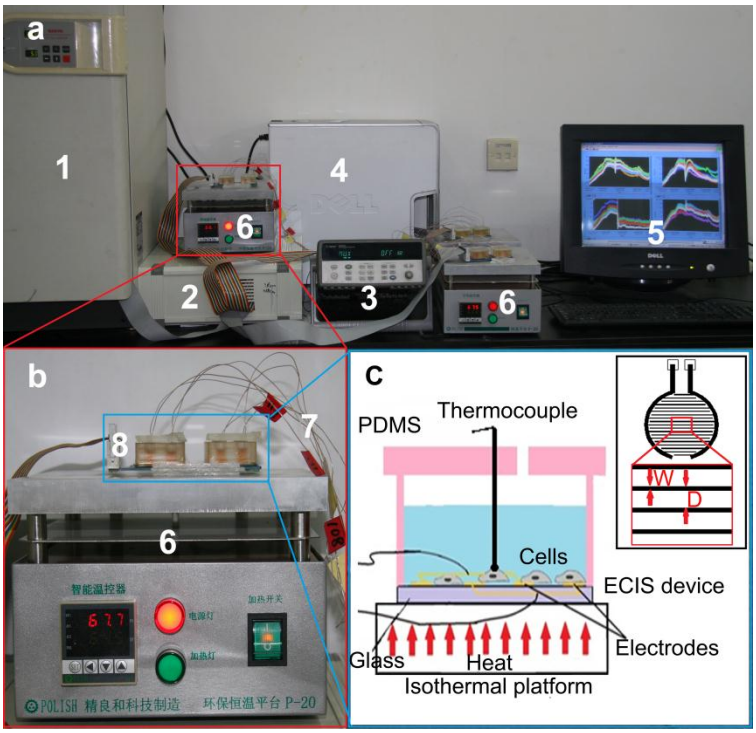


**Figure 1.** The experimental platform (a) with highlight pictures of the treatment set-up (b) and the details of ECIS device with temperature sensing function (c). (1) Incubator, (2) amplifying circuit, (3) Agilent 34970A, (4) PC host, (5) software interface, (6) isothermal plate, (7) thermocouples, and (8) ECIS device. Insert of (c) shows the details of a pair of interdigital electrodes, width (W)=20 μm, distance (D)=100 μm. Cells were seeded in the cavities of the ECIS device (8), whose inside substrate was covered with interdigital gold electrodes. The ECIS devices were connected to the amplifying circuit (2), which was controlled by the computer (4). Cells spread and proliferated on the electrodes, and thus, the impedance between electrodes could be detected. Heat in the cell culture cavity was generated by the isothermal plate (6), and the thermocouples (7) were set in the culture medium to measure the temperatures in real-time. A computer (4) was utilized to control the ECIS system and Agilent 34970A (3), as well as to process the impedance and temperature data.

The thermocouples were calibrated with an ice water mixture, and the temperature inputs of different channels were simultaneously acquired by an Agilent data acquisition/switch unit 34970A, while continuously processed by the accompanying software. All the temperatures of the 32 wells were controlled automatically around the setting range (with an accuracy of 0.5 ℃) by the thermocouples and PID controlling system. The impedance and temperature data were eventually collected and processed on the PC. Tests on the devices showed that the impedance variations between electrodes covered with culture medium (DMEM) alone during hyperthermia were negligible compared to that covered with adherent cells and culture medium (see in Fig. S1). Thus the whole platform can provide rapid impedance sensing as well as accurate and stable temperature controlling function, which is suitable for *in vitro* hyperthermia research.

## 2.4 Experimental procedures for in vitro hyperthermia assays

All instruments and tools were sterilized and placed in a clean room. The ECIS devices were carefully washed with phosphate buffered saline (PBS), dried by nitrogen, and then sterilized in a high-pressure sterilizer (SANYO Electric Biomedical Co., Ltd, Osaka, Japan) and air-dried on a super clean bench. DMEM medium (200 μL) was added to the ECIS device and incubated at 37 °C for 20 min to record the culture medium's background impedance module ($Z_b$, ~32 Ω). Then, medium containing cells (400 μL) was seeded randomly into each cell culture cavity of the ECIS device at a final density of $1\times10^5$ cells/mL and cultured at 37 ℃ in a standard cell culture incubator. The devices were connected to the amplifying circuit for continuous impedance monitoring. The impedance module ($Z_x$) was

measured at 60 KHz with a sinusoidal voltage of 10 mV every 5 min and displayed in real time by the self-developed software. The frequency and amplitude of the stimulate voltage were optimized in our previous publication[38].

When the impedance curves showed that the cell proliferation had reached its plateau stage (incubated for ~24 h), the experimental ECIS devices were taken out of the incubator and placed on the isothermal plates; the control ECIS device was kept in the incubator. The isothermal plates were adjusted to ensure temperatures around the cells in the ECIS devices were 41, 43, or 45 ℃, and maintained for 30 min, respectively. All cavities were simultaneously monitored by the ECIS system and the thermocouples during the hyperthermia process. Temperatures were measured every 2 s, and the impedances of all channels were measured every 16 s.

After the treatment, the devices were placed back into the incubator and monitored by the ECIS system for ≥ 24 h. The interval of impedance detection was changed back to 5 min. The impedance module at the beginning of the hyperthermia ($Z_0$, 60-70 Ω) was set as a baseline, and the final impedance data were normalized as $(Z_x-Z_b)/(Z_0-Z_b)$ to reduce the effect of background impedance.

## 2.5 Comparison of ECIS with fluorescent labeling, MTT assays, and morphological observation

### 2.5.1 Fluorescence labeling

Annexin-V-FITC/PI staining assays were used to classify cells in the early apoptosis and late apoptosis/dead stages. For fluorescence imaging, 1 mM PI and 4 mM Annexin V-FITC were added to the cell mixture for 30 min at 37 ℃. After washing with PBS, cells were

imaged using a fluorescence microscope (DM-IRB, Leica, Solms, Germany) with a CCD camera (DP-71, Olympus, Tokyo, Japan).

### 2.5.2 MTT assays

A549 cell suspension (200 μL of $1\times10^5$ cells/mL) was seeded in each well of a 96-well plate. After a 24-h incubation, the cells' growth reached its plateau stage and cells were treated with the above-mentioned *in vitro* hyperthermia assays. Then, cells in different 96-well plates were placed back into the incubator for different additional culture periods: control, and 0, 1, 4, 8, 12, 16, 20, and 24 h after hyperthermia. At the end of the incubation, 20 μL PBS with 5 mg/mL MTT were added to each well for a 4-h incubation. Next, 150 μL DMSO solution was added, and the culture plates were shaken on an orbital shaker at room temperature for 10 min. Finally, the optical density of each sample was measured at 490 nm with a spectrophotometer (Model 680, Bio-Rad, Shanghai, China). The control experiment was conducted by the same process just before the hyperthermia treatment started.

### 2.5.3 Morphological observation

A549 cells (suspension of $1\times10^3$ cells/mL) were seeded in a Petri dish (diameter = 30 mm) and cultured in an incubator at 37 ℃ for 12 h. Then, the Petri dish was heated by an Indium Tin Oxide (ITO) glass, and the temperature was monitored with a PID controller using a thermocouple. The Petri dish and the ITO glass were placed on a cell imaging system (DeltaVision, General Electric Co., Fairfield, CT) for morphological observation (see in Fig. S3). The same ranges of cells were similarly treated as in the in vitro hyperthermia experiment as described before, and imaged every 16 s during the whole hyperthermia process and 1 h afterwards.

# Results and Discussions

## 3.1 Dynamic impedance monitoring of the cellular response to hyperthermia and fluorescence labeling results

Our platform was used to monitor hyperthermia-induced changes in A549 cells over 48 h and the impendence data were compared with data obtained from standard fluorescence labeling, MTT assays and morphological observation at several discrete time points. A normalized impedance curve is shown in Figure 2a. During the 30-min hyperthermia treatment at 43 ℃, the impedance value ($Z_{43\ ℃}$) increased to 1.2 at the beginning of the treatment, and then decreased sharply to ~0.4. After the treatment, the $Z_{43\ ℃}$ slowly recovered to approximately 1.2 during the following 8 h, where it remained for several hours before ultimately slowly decreasing again. These observations were independently verified by fluorescent imaging, as shown in Figure 2b–d. Bright-field and fluorescent images are shown, at four time points: 0, 1, 8, and 24 h after a 43 ℃ treatment for 30 min. Early apoptotic cells are stained by Annexin V-FITC (green fluorescence), while dead or late-stage apoptotic cells are stained with PI (red fluorescence), the quantitative results were shown in Table 1. At the 0, 1, and 8 h time points after treatment, the impedance ($Z_{43\ ℃}$) decreased and recovered noticeably (Fig. 2a), but rare cells were stained by PI/Annexin V-FITC. At the 24-h time point after treatment, the number of PI/Annexin V-FITC stained cells significantly increased, indicating that an increased number of cells underwent apoptosis. The staining results correlated well with the impedance curve during the 8-24 h interval after treatment, demonstrating that the ECIS method could monitor slow cell status changes (such as apoptosis). The gene expression results of heat shock protein (HSP) related genes (Fig. S2)

showed that the HSP expression level increased at least 20 min after treatment started, and reached a maximum value at 8 h after treatment. This indicated that the cell's stress response to heat activated at early stage, thus the decrease and recovery of impedance from hyperthermia to 8 h after treatment demonstrated that the ECIS results also reflect rapid thermal-induced cell changes (possibly stress reactions) at early stages. These were likely not caused by apoptosis or necrosis and hence cannot be measured by fluorescence labeling.

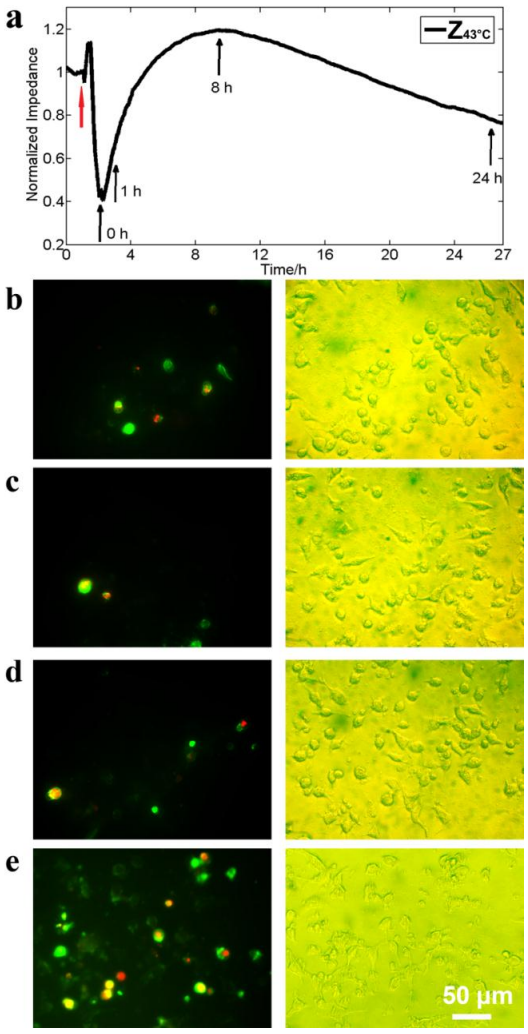


**Figure 2.** Impedance profiling *vs.* staining results of A549 cells. (a) Impedance curve of A549 cells under 43 ℃ hyperthermia ($Z_{43℃}$) for 30 min (the red arrow indicates the start-time of the treatment). (b-e) Apoptosis staining (Annexin-V-FITC/PI staining) results at different time points (0, 1, 8, and 24 h) after hyperthermia (left column: fluorescence labeling results,

green and red fluorescence represent cells stained by Annexin-V-FITC and PI, respectively. Right column: bright field images of the same range as the left ones).

Table 1 Cells that uptake Annexin-V or PI compared to total (cell/mm$^2$)

| Time point (h) | Annexin-V | PI | Total |
|---|---|---|---|
| 0 | 7 (97.2) | 4 (55.6) | 61 (847.2) |
| 1 | 4 (55.6) | 2 (27.8) | 63 (875.0) |
| 8 | 13 (180.6) | 5 (69.4) | 65 (902.8) |
| 24 | 33 (458.3) | 11 (152.8) | 60 (833.3) |

## 3.2 Correlation analysis between the impedance data and MTT assays

The impedance detection results were compared to data from MTT assays determined at 24 h after treatment at different temperatures (41 , 43 , and 45 ℃) for 30 min and at various time points (control, and 0 h, 1, 4, 8, 12, 16, 20, and 24 h after hyperthermia) for the 43 ℃ treatment for 30 min. Figure 3a shows the impedance curves of A549 cells after different hyperthermia treatments. The impedance of the experimental groups obviously decreased during hyperthermia, and the range of the decrease depended on the temperature and treatment time. The measured cellular impedance of 41 ℃ and 43 ℃ groups both recovered after treatment, but the impedance in the 41 ℃ group ($Z_{41\ ℃}$) recovered more quickly than that in the 43 ℃ group ($Z_{43\ ℃}$). The $Z_{43\ ℃}$ then again decreased after 8 h of incubation, while the impedance of the control cells ($Z_{ctr}$) presented no obvious change until 24 h after treatment. In particular, the relative cellular impedance decreased to ~0.2 and was maintained at this low level until 24 h after exposure to a 45 ℃ hyperthermia treatment for 30 min, indicating that only a small portion of the cells were viable and adhered to the ECIS device surface.

MTT assays were performed to determine the temperature-dependent cytotoxicity of

hyperthermia as a standard comparison method. For comparison of cells treated by different temperatures, the viability of A549 cells was assessed by MTT assays at 24 h after exposure to four different temperatures within 30 min (the arrow in Fig. 3a highlights the comparison time point). Further, the MTT values were normalized by establishing the control value (without hyperthermia) as 1. The correlation analysis between the MTT assays and the impedance data is presented in Figure 3c. The high correlation efficiency ($R^2$ = 0.9873) indicates a close agreement between the standard MTT assays and the ECIS system detection. For the time-dependent measurements after treatment, A549 cells were exposed to 43 ℃ for 30 min, and MTT assays were performed at nine different time-points before and after treatment. We also normalized the MTT values by setting the value at 0 h before treatment as 1 (Fig. 3b). As shown in Figure 3b, it is clear that the measured MTT values do not agree with the impedance values during treatment, but the trends at the later time points are highly correlated with impedance curve. The correlation analysis (Fig. 3d) of MTT and impedance values at the final six time points (4, 8, 12, 16, 20, and 24 h after hyperthermia treatment) displayed a high correlation efficiency ($R^2$ = 0.949). These results demonstrated that MTT assays can monitor the cell apoptosis/necrosis that identified by the ECIS system but cannot identify rapid cell changes evident in the impedance curves during and after hyperthermia. The moderate decrease of MTT values during hyperthermia indicated that the cells' viability was not destroyed as severely as the impedance curve ($Z_{43\ ℃}$) showed.

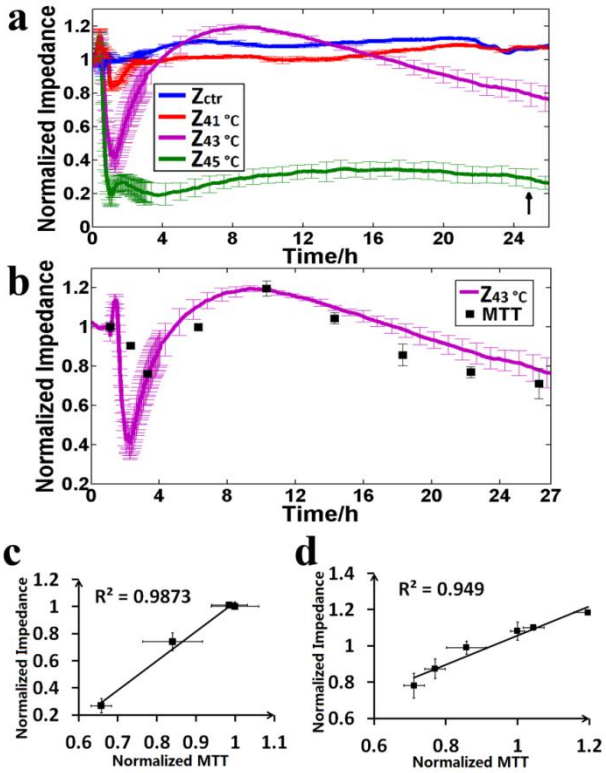


**Figure 3.** Impedance profiling of A549 cells undergoing hyperthermia *vs.* control cells and correlation analysis of MTT data with impedance. (a) Impedance profiling of A549 cells undergoing 41, 43, and 45 ℃ hyperthermia for 30 min *vs.* controls. The treatments were started at 0 h ($Z_{ctr}$, $Z_{41\ ℃}$, $Z_{43\ ℃}$, and $Z_{45\ ℃}$ stand for the impedance of cells under 37 ℃ in the incubator or 41, 43, and 45 ℃ hyperthermia for 30 min, respectively. The same applies for the rest of the figures). (b) Normalized MTT value and normalized impedance value of A549 cells undergoing 43 ℃ hyperthermia; both normalize the value of 0 h before hyperthermia as 1. (c) The correlation index of MTT data and impedance data at time 24 h after hyperthermia (the arrow in Figure 3a indicates the time point of the correlation). (d) The correlation index of the last six time points of MTT data with the impedance data of A549 cells undergoing 43 ℃ hyperthermia after treatment had finished for 4 h.

## 3.3 Verifying impedance data with continuous morphological observations

As fluorescence labeling and the MTT method did not reflect the rapid cell status changes during hyperthermia as shown in the impedance curves, and Jen *et al.* report that morphology changes occur rapidly in thermal-treated cells, we hypothesized that cell morphology changes caused the rapid impedance loss during hyperthermia. To test this hypothesis, a cell imaging system and a heating device were used to assess the morphological changes during and after hyperthermia (S3). We independently assessed the morphology of A549 cells during and 1 h after hyperthermia treatments (37, 41, 43, and 45 ℃ for 30 min) and the images were composed into supplementary videos (Video S4-S7). The morphology images in response to different temperatures at discreet time points are shown in Figure 4. Figure 4a shows the impedance curves of A549 cells under different hyperthermia treatments (highlight of the first 2 h in Fig. 3a), and the arrows marked 1, 2, 3, and 4 indicate the time points at which the photos were taken. Figure 4b-e are micrographs of the four time points during the 37 ℃ incubation, and 41, 43, and 45 ℃ hyperthermia treatments, respectively. These data clearly demonstrated that cellular morphology changed little during the 37 ℃ incubation but severely during the hyperthermia treatments. Cells began to shrink once the treatments began, corresponding to fluctuation of the impedance curves. At the end of the treatment (time point (3)), part of the cells in the 41 ℃ and the majority of the cells in 43 ℃ treatment groups became round (Fig. 4c and Fig. 4d). After hyperthermia, cells in the 41 ℃ group quickly spread on to the substrate forming irregular fusiform shapes (time point of 4 in Fig. 4c), and cells in the 43 ℃ group did not show an obvious spreading process (time point (4) in Fig. 4d). The cells in the 45 ℃ group also shrank quickly, although less obviously than in the 43 ℃ group (time points (2) and (3) in Fig. 4e). At the later phase of hyperthermia,

cells began to 'burst' one by one until the last observation (time points of (3) and (4) in Fig. 4e). This 'burst' process is clearly shown in the Supplementary Video (S6). Subsequently, cells in the 45 ℃ hyperthermia group no longer changed, and all of the 'burst' cells could be stained by PI (Fig. S8). These results demonstrated that this rapid change of cell status was necrosis. The impedance curves of the 41, 43, and 45 ℃ groups (Fig. 4a) demonstrated similar dynamic fluctuations during and after hyperthermia. After a temperature- and time-dependent decrease, the impedance in the 41 ℃ group quickly recovered to ~1 in 1-2 h, while it required 7-8 h in the 43 ℃ group. Moreover, those cells in the 45 ℃ group displayed no obvious recovery. These results demonstrated that the rapid loss and recovery of impedance was highly relevant to morphologic change, and our ECIS system succeeded in providing a comparable sensitivity and resolution to that of a cell imaging system.

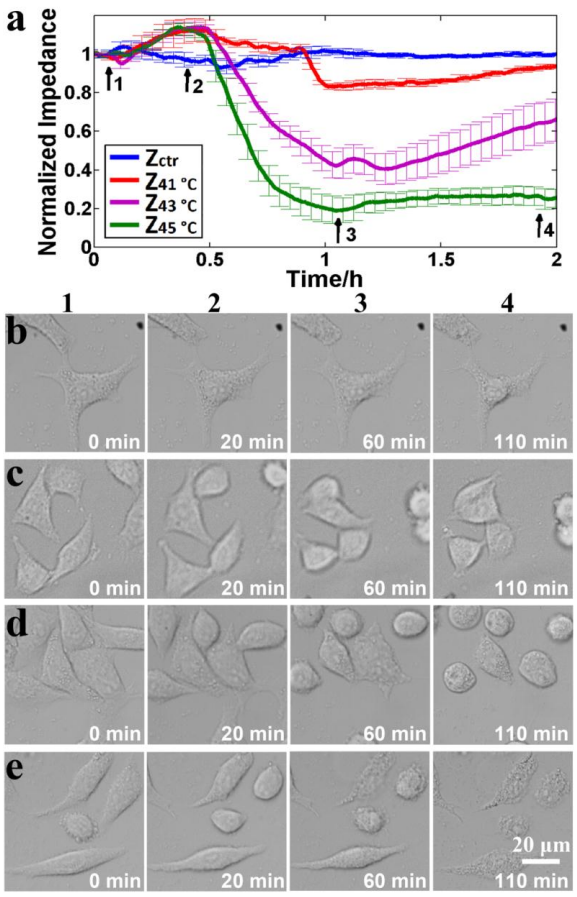

**Figure 4.** Highlight of impedance (a) and morphological changes (b-e) of settled ranges of cells during and 1 h after hyperthermia for 30 min at different temperatures (b-e represent 37, 41, 43, and 45 ℃ respectively). (b-e) From left to right: images at the time points of (1), (2), (3), and (4), which were 0 min (begin heating), 20 min after heating initiated, the end of hyperthermia, and 1 h after the end of hyperthermia, respectively. Videos demonstrating the detailed process are available in the supplementary data (Videos S4-S7).

From these three types of verifying experiments over A549 cells, we demonstrated that the rapid changes of cell morphology and necrosis, as well as slow variations of cell status including apoptosis, can be quantitatively detected by ECIS in real time. For cells treated at 43℃ for 30 min, this rapid loss of impedance corresponded with morphology changes followed by a process of recovery (possibly self-repairing) and a slowly decrease after recovery, which was possibly caused by apoptosis. We also demonstrated that 45 ℃ hyperthermia for 30 min leads to a fast and deep decrease of impedance followed by no obvious recovery, likely due to necrosis after hyperthermia. It seems that the rapid cell status changes during and after hyperthermia are important processes for cell stress reaction and self-repair, including pro-apoptotic/necrotic processes.

The comparison of results demonstrated that both the florescence labeling and morphological observation methods cannot provide quantitative results, and the MTT assay could not accurately monitor the rapid changes during hyperthermia. Furthermore, despite the fluorescence labeling, MTT assays could be performed at additional time points, but the costs and significantly increased experimental efforts cannot be disregarded. In contrast, the ECIS

method provides multiple cavities for continuous measurement over parallel groups of small numbers of cells and sensitively detects rapid cell changes within 16 s. The continuous and sensitive measurement afforded by the ECIS system provided better temporal resolution for cell status changes. Compared to the traditional endpoint measurements, this approach tremendously reduces the detection intermediate time. Similarly, compared to morphological observation via microscopy, our platform can provide sensitivity and quantitative results, which turn out to be more helpful for thermal sensitivity analysis.

## 3.4 ECIS profiling of the thermal sensitivities of the human liver cell lines LO2 and HepG2

Hyperthermia is mainly based on the theory that tumor cells are more thermal-sensitive than normal cells[39, 40]. Therefore, cancer cells should be more vulnerable to apoptosis or necrosis than normal cells when exposed to high temperatures. To test this hypothesis, we evaluated the thermal sensitivities of LO2 and HepG2 cells using our platform (LO2 and HepG2 are typical human normal and tumorous liver cell lines). The impedance curves are shown in Figure 5 with highlights of curves during hyperthermia. The impedance curves of LO2 (Fig. 5a and Fig. 5c) showed that, compared to the control group, the 41 ℃ and 43 ℃ hyperthermia treatments for 30 min caused loss and recovery of impedance curves in 2-6 h but did not change the long-term trend in the subsequent after-treatment incubation. The normalized impedance value recovered to ~1 at 2 h (41 ℃ group) and 8 h (43 ℃ group) post-treatment, and then remained at a value comparable to the control group up to 24 h after hyperthermia. Only the 45 ℃ hyperthermia group showed an obvious loss of impedance 24 h after hyperthermia. Although impedance obviously recovered during the time frame 0-8 h

after treatment, it ultimately decrease after reaching a maximum value of 0.7 while the control showed only minor changes. According to aforementioned results (Fig.1-3), we deduced that the cells in 45 ℃ group likely experienced apoptosis, and no obvious necrosis occurred in any of the hyperthermia-treated LO2 groups.

The impedance curves of HepG2 cells (Fig. 5b and Fig. 5d) showed similar results when compared to A549 cells. After treatment, impedance recovered in the 41 ℃ and 43 ℃ groups, however the impedance in the 45 ℃ group showed no obvious increase after treatment. The impedance of the 43 ℃ group ($Z_{43\ ℃}$) then decreased after 24 h of incubation, while the impedance curves of the control ($Z_{ctr}$) and the recovered 41 ℃ group ($Z_{41\ ℃}$) did not change until 44 h after treatments. This indicates that the 43 ℃ hyperthermia treatment for 30 min was severe enough to promote apoptosis of the HepG2 cells, and the 45 ℃ treatment lead to necrosis. The impedance trend of the LO2 cells treated at 45 ℃ for 30 min was similar to that of HepG2 cells treated at 43 ℃ for 30 min (decrease-recover-decrease), indicating the possible threshold to apoptosis for LO2 may be up to 45 ℃. A result of another normal cell line (HaCaT) showed similar patterns to LO2 in 41 and 43 ℃ hyperthermia, meaning the threshold of apoptosis for HaCaT must be >43 ℃ (Fig. S9) and the higher threshold (>43 ℃) may be generally existed in normal cell lines. Hence, we concluded that the cancer cell line HepG2 is more sensitive to hyperthermia and thus could be damaged by heat more easily than LO2 cells. Our results fit the published literature, and this threshold difference should be helpful for clinic utilization of hyperthermia in liver cancer treatment[39].

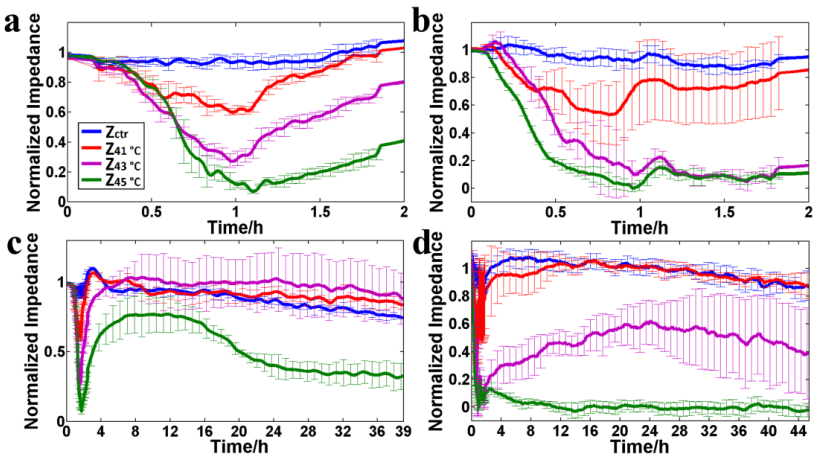


**Figure 5.** Dynamic impedance curves (37 ℃ as a control, or 41, 43, and 45 ℃ hyperthermia for 30 min, respectively, the same for Figure 6) during and after hyperthermia for the LO2 and HepG2 cell lines. (a) and (b) Impedance curves of LO2 and HepG2 cells during hyperthermia, respectively. (c) and (d) Impedance curves of LO2 and HepG2 cells after hyperthermia, respectively.

## 3.5 Evaluation of the thermal sensitivity of different cancer cell lines by impedance profiling

Although 43 ℃ is widely accepted as a common threshold of apoptosis for various cancer cells, many reports indicate that different thermal sensitivities exist among different cell lines[9, 10]. Thus, we evaluated four typical cancer cell lines (HeLa, MCF-7, HepG2, and A549) using our experimental platform. Figure 6 shows the impedance curves during and after hyperthermia. When the heating process began, the impedance of HeLa, MCF-7, and HepG2 cells (Fig. 6a-c, respectively) decreased, while the A549 cell's impedance (Fig. 6d) gently increased to 1.2 in 20 min and then decreased. These short-term impedance changes of the A549 cells were likely caused by the cells' stress reaction. The curves of the 41 °C and 45 ℃ groups in the different cell lines demonstrated similar tendencies after treatment (Fig.

429 6e-f). In the 41 ℃ treatment group, the impedance decreased by ~0.2 after treatment and
430 quickly recovered to ~1 in 1-2 h, when it was then maintained as in the control group. In the
431 45 ℃ treatment group, the impedance decreased by ~0.8-1 after treatment, and did not
432 recover during subsequent incubation. The similarities between the results of the 41 ℃ and
433 45 ℃ treatment groups demonstrated that different cell lines share the same hyperthermia
434 mechanisms under these temperatures. First, hyperthermia caused an impedance decrease
435 (possibly stress reactions), and the range was determined by the treatment temperature and
436 time. Although the 41 ℃ hyperthermia for 30 min treatment can cause an obvious impedance
437 loss, cells quickly recovered to normal levels (possibly self-repairing). For all four cell lines,
438 the 45 ℃ hyperthermia for 30 min treatment caused immediate and severe damage (possibly
439 necrosis) that was not repaired during subsequent incubation.

440 For the 43 ℃ treatment group, the impedance curves of the four cell lines also displayed
441 some common tendencies. Their impedance curves sharply decreased during hyperthermia,
442 recovered in several hours, and then slowly decreased again. Based on the results in Figures 2
443 and 3, we hypothesize that all four cell lines were severely damaged and underwent apoptosis
444 after heat treatment. However, there were distinctive impedance changes among four cell
445 lines. The HeLa cell impedance decreased by ~0.6 during hyperthermia and then recovered to
446 0.9-1 in 8 h, following the same trend as the control group until the end of the experiment.
447 The HepG2 cell impedance decreased by 0.8 and recovered to ~0.6 in 24 h, and then slowly
448 decreased. For the A549 cell line, the impedance value decreased by 0.6, strongly recovered
449 to 1.2 in 8 h, and then decreased much more quickly than the control. For the MCF-7 cell line,
450 the impedance decreased by 0.6 during hyperthermia, recovered to ~0.7 in 8 h, and then

gradually decreased. Therefore, we concluded that all four cell lines were affected by the hyperthermia treatment, partially recovered their viability, and then subsequently underwent apoptosis. The dynamic results of the 43 ℃ treatment demonstrate that different cell lines display different impedance changes, indicating that different thermal sensitivities exist among them. For instance, the A549 cells displayed a stronger stress reaction and self-repair process than other cell lines, and the HepG2 cells displayed a longer self-repair time than other cell lines.

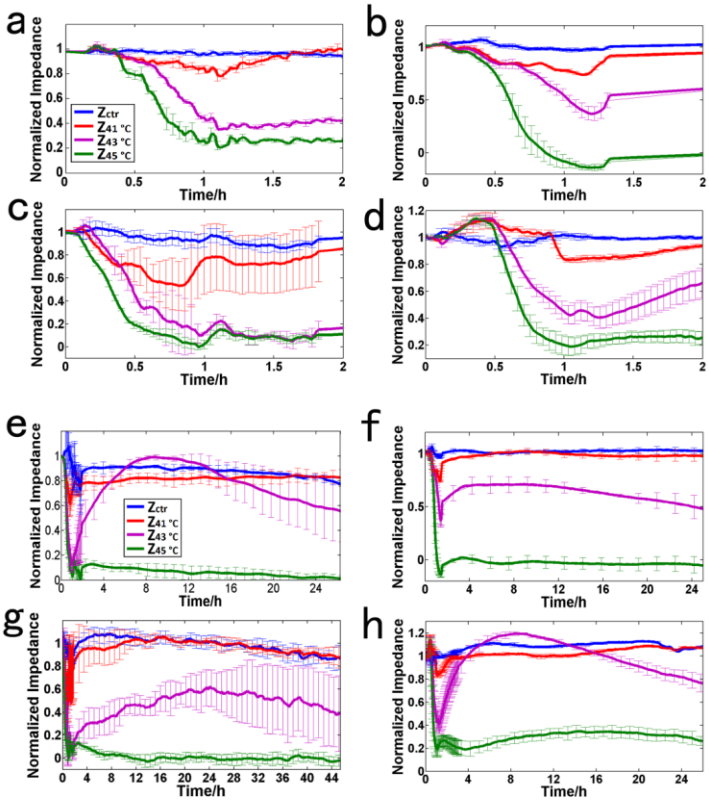


**Figure 6.** Dynamic impedance curves of different cell lines (HeLa, MCF-7, HepG2 and A549) during (a-d) and after hyperthermia (e-h). (a, e) HeLa cells, (b, f) MCF-7 cells, (c, g) HepG2 cells, and (d, h) A549 cells.

Typical changes in impedance tendencies reflecting different treatment effects existed

among the five investigated cell lines' impedance profiling results. The $Z_{41\ ℃}$ of all five cell lines displayed a minor impedance decrease and almost completely recovery subsequently (a "V" shape tendency), indicating cell stress reactions caused by the heat. The $Z_{43\ ℃}$ of the HeLa, MCF-7, HepG2, and A549 cell lines exhibited a sharp decrease, slow recovery for several hours and slower ultimate decrease (a "r" shape tendency), possibly implying the processes of stress reactions, self-repair, and apoptosis, respectively. The $Z_{45\ ℃}$ of all four cancer cell lines (HeLa, MCF-7, HepG2, and A549) demonstrated a sharp decrease with no obvious recovery until 24 h (a "L" shape tendency), which most likely represented necrosis caused by the hyperthermia. These three typical impedance curves exhibited three consequences under low, middle, and high dose/time combinations of hyperthermia. Previous researches prove that both apoptosis and necrosis have certain threshold temperatures[41, 42], which are approximately 43 ℃ and 45 ℃ [43], respectively. Thus, our results correspond very well with published data.

Based on the trends of the impedance curves, we postulated possible response mechanisms occurring in the cells. These common phenomena indicated that the same/similar mechanisms are enacted in response to hyperthermia in cancer cell lines. However, there were differences in dynamic impedance results for the 43 ℃ hyperthermia treatment, demonstrating the diversity of thermal sensitivities in various cancer cell lines. Synthetically, the temperature threshold of these four cancer cells for (likely) apoptosis was approximately 43 ℃, but a few differences exist in different cancer cell lines (possibly the differences in treatment time/interval needed). Regardless, based on the impedance curves, we deduced that the apoptosis threshold differences in these four cancer cell lines will not exceed the

difference of thresholds between the LO2 and HepG2 cell lines.

## Conclusions

In this study, we constructed an ECIS-based platform to dynamically monitor cell status before, during, and after heat exposure, and our results are consistent with a series of theories on hyperthermia treatment and comparable with conventional assay methods. The highlight of our research is impedance curves that can reveal subtle and rapid changes of cell status during and after hyperthermia, which may indicate the dynamic biological processes that occur in cells in response to hyperthermia, such as stress reactions, self-repair, apoptosis, or necrosis. Using this platform, five types of cells, including normal and cancer cells were investigated, presenting different thermal sensitivities during hyperthermia treatment. These results demonstrated that our platform is a useful analytical tool to study hyperthermia *in vitro*, providing the strong possibility of discovering new mechanisms and screening treatment-enhancing methods. Considering ECIS technique's previous applications to screening drugs for chemotherapy[35], this platform also has the potential to research and optimize thermo-chemotherapy.

## Supporting Material

Five figures and four videos are available in ***Supporting Material***.

## Acknowledgements

This research was supported by the National Scientific Equipment Development Special Foundation of China under Grant No. 2011YQ030134, and the Foundation of Beijing

Laboratory in Biomedical Technology and Instrument.

# References


1. D. S. Coffey, R. H. Getzenberg and T. L. DeWeese, *JAMA*, 2006, 296, 445-448.
2. E. L. Jones, J. R. Oleson, L. R. Prosnitz, T. V. Samulski, Z. Vujaskovic, D. Yu, L. L. Sanders and M. W. Dewhirst, *Journal of Clinical Oncology*, 2005, 23, 3079-3085.
3. M. Dewhirst, B. Viglianti, M. Lora-Michiels, M. Hanson and P. Hoopes, *International Journal of Hyperthermia*, 2003, 19, 267-294.
4. W. C. Dewey, *International Journal of Hyperthermia*, 2009, 25, 3-20.
5. E. Jones, D. Thrall, M. W. Dewhirst and Z. Vujaskovic, *International journal of hyperthermia : the official journal of European Society for Hyperthermic Oncology, North American Hyperthermia Group*, 2006, 22, 247-253.
6. L. Roizin-Towle and J. P. Pirro, *International Journal of Radiation Oncology* Biology* Physics*, 1991, 20, 751-756.
7. J. L. Roti Roti, *International Journal of hyperthermia*, 2008, 24, 3-15.
8. C. P. Jen, C. T. Huang and C. H. Tsai, *Annals of biomedical engineering*, 2009, 37, 2407-2415.
9. C. U. Lim, Y. Zhang and M. H. Fox, *International journal of hyperthermia : the official journal of European Society for Hyperthermic Oncology, North American Hyperthermia Group*, 2006, 22, 77-91.
10. Y. G. Shellman, W. R. Howe, L. A. Miller, N. B. Goldstein, T. R. Pacheco, R. L. Mahajan, S. M. LaRue and D. A. Norris, *Journal of Investigative Dermatology*, 2007, 128, 949-956.
11. G. Hegyi, G. P. Szigeti and A. Szász, *Evidence-Based Complementary and Alternative Medicine*, 2013, 2013 %@ 1741-427X.
12. B. Hildebrandt, P. Wust, O. Ahlers, A. Dieing, G. Sreenivasa, T. Kerner, R. Felix and H. Riess, *Critical reviews in oncology/hematology*, 2002, 43, 33-56.
13. J. Zhou, X. Wang, L. Du, L. Zhao, F. Lei, W. OuYang, Y. Zhang, Y. Liao and J. Tang, *Molecular medicine reports*, 2011, 4, 187-191 %@ 1791-2997.
14. D. Simanovskii, M. Mackanos, A. Irani, C. O'Connell-Rodwell, C. Contag, H. Schwettman and D. Palanker, *Physical Review E*, 2006, 74, 011915.
15. S. Bhowmick, J. E. Coad, D. J. Swanlund and J. C. Bischof, *International journal of hyperthermia : the official journal of European Society for Hyperthermic Oncology, North American Hyperthermia Group*, 2004, 20, 73-92.
16. T. Curry, T. Epstein, R. Smith and R. Kopelman, *Nanomedicine*, 2013, 8, 1577-1586.
17. D. D. Mosser, A. W. Caron, L. Bourget, C. Denis-Larose and B. Massie, *Molecular and cellular biology*, 1997, 17, 5317-5327.
18. C.-M. Lo, C. R. Keese and I. Giaever, *Biophysical journal*, 1995, 69, 2800.
19. K. C. Klamer SE, Hordijk PL, et al. , *Cell Adhesion & Migration*, 2013, 5, 434–449.
20. I. Voiculescu, F. Li, F. Liu, X. Zhang, L. M. Cancel, J. M. Tarbell and A. Khademhosseini, *Sensors and Actuators B: Chemical*, 2013, 182, 696-705.
21. T. A. Nguyen, T.-I. Yin, D. Reyes and G. A. Urban, *Analytical chemistry*, 2013, 85, 11068-11076.
22. D. Bennet and S. Kim, *Analytical chemistry*, 2013, 85, 4902-4911.
23. L. Wang, L. Wang, H. Yin, W. Xing, Z. Yu, M. Guo and J. Cheng, *Biosensors & bioelectronics*, 2010, 25,

990-995.
24. H. Yin, F. L. Wang*, A. L. Wang, J. Cheng and Y. Zhou, *Analytical Letters*, 2007, 40, 85-94.
25. L. Wang, J. Zhu, C. Deng, W. L. Xing and J. Cheng, *Lab on a chip*, 2008, 8, 872-878.
26. V. Yarotskyy and R. T. Dirksen, *Biophysical journal*, 2012, 103, 202-211.
27. R. T. Dirksen and G. Avila, *Biophysical journal*, 2004, 87, 3193-3204.
28. L. Otero-González, R. Sierra-Alvarez, S. Boitano and J. A. Field, *Environmental science & technology*, 2012, 46, 10271-10278.
29. M. Tarantola, D. Schneider, E. Sunnick, H. Adam, S. Pierrat, C. Rosman, V. Breus, C. Sonnichsen, T. Basché and J. Wegener, *Acs Nano*, 2008, 3, 213-222.
30. P. O. Bagnaninchi and N. Drummond, *Proceedings of the National Academy of Sciences*, 2011, 108, 6462-6467.
31. T. B. Tran, S. Cho and J. Min, *Biosensors and Bioelectronics*, 2013, 50, 453-459.
32. Y. Xu, Y. Lv, L. Wang, W. Xing and J. Cheng, *Biosensors & bioelectronics*, 2012, 32, 300-304.
33. M. Fox, D. Esveld, A. Valero, R. Luttge, H. Mastwijk, P. Bartels, A. Van Den Berg and R. Boom, *Analytical and bioanalytical chemistry*, 2006, 385, 474-485.
34. J. A. Stolwijk, C. Hartmann, P. Balani, S. Albermann, C. R. Keese, I. Giaever and J. Wegener, *Biosensors and Bioelectronics*, 2011, 26, 4720-4727.
35. F. Xie, Y. Xu, L. Wang, K. Mitchelson, W. Xing and J. Cheng, *The Analyst*, 2012, 137, 1343-1350.
36. Y. Zhang, H. Wang, L. Wang and J. Cheng, *Analytical Letters*, 2012, 45, 1045-1057.
37. Y. Zhang, L. Wang, J. Zhu, Y. Hu, W. Xing and J. Cheng, *Biotechnology letters*, 2012, 34, 397-404.
38. L. Wang, H. Wang, L. Wang, K. Mitchelson, Z. Yu and J. Cheng, *Biosensors & bioelectronics*, 2008, 24, 14-21.
39. A. Chicheł, J. Skowronek, M. Kubaszewska and M. Kanikowski, *Reports of Practical Oncology & Radiotherapy*, 2007, 12, 267-275.
40. Y. Sakaguchi, L. C. Stephens, M. Makino, T. Kaneko, F. R. Strebel, L. L. Danhauser, G. N. Jenkins and J. M. Bull, *Cancer research*, 1995, 55, 5459-5464.
41. B. Harmon, A. Corder, R. Collins, G. Gobe, J. Allen, D. Allan and J. Kerr, *International journal of radiation biology*, 1990, 58, 845-858.
42. M. Yonezawa, T. Otsuka, N. Matsui, H. Tsuji, K. H. Kato, A. Moriyama and T. Kato, *International journal of cancer*, 1996, 66, 347-351.
43. R. D. Issels, *European journal of cancer*, 2008, 44, 2546-2554.